Effect of Deformation on the Microstructure and General Corrosion Behavior of Alloy 690TT Tube in Steam Generator Crevices

Soon-Hyeok Jeon [a,*], Ji-Young Han [a,b], Do Haeng Hur [a], Hee-Sang Shim [a], Sung-Woo Kim [a]
[a]*Materials Safety Technology Research Division, Korea Atomic Energy Research Institute, Daejeon, 34057, Korea*
[b]*Department of Materials Science and Engineering, Yonsei University, Seoul, 03722, Korea*
[*]*Corresponding author: junsoon@kaeri.re.kr*

Keywords : steam generator, Alloy 690, deformation, microstructure, corrosion, crevice

1. Introduction

Recently, Alloy 690 material, which has better corrosion resistance than Alloy 600, is widely used as a steam generator (SG) tube in nuclear power plants. Nevertheless, there still remains a potential problem that could damage the SG tubes. Notably, there are some dented tubes even in SGs with Alloy 690 thermally treated (TT) tubes [1,2].

Denting phenomenon is another type of damage that affect the SG integrity, although it is not directly related to corrosion of the SG tube itself. SG tube denting is defined as the reduction in tube diameter due to the volume expansion of the corrosion products formed by continuous corrosion of the top-of-tubesheet (TTS) or tube support plate (TSP) in SG crevices [3].

Fig. 1 shows the TTS denting mechanism of SG crevices in PWRs. With the passage of time, the corrosion process converts the tubesheet (TS) surface into the corresponding oxide form. For the TS material, which is typically a low alloy steel such as SA508 and SA533 with limited corrosion resistance, the volume of the corrosion products is larger than that of the metal from which is formed. The volume of magnetite (Fe_3O_4) is about 2.4 times that of the iron from which it forms [4]. The corrosion acceleration of the TS leads to the packing of the TTS crevice with corrosion products and could result in the imposition of compressive stress on the outer diameter of the SG tubes [4]. In recent SG, the thickness of the crevice gap between the expanded SG tube and TS is about 4 mils radially or 8 mils diametrically. Corrosion penetration of about 2.9 mils into the TS could produce the sufficient corrosion products to fill the TTS crevice.

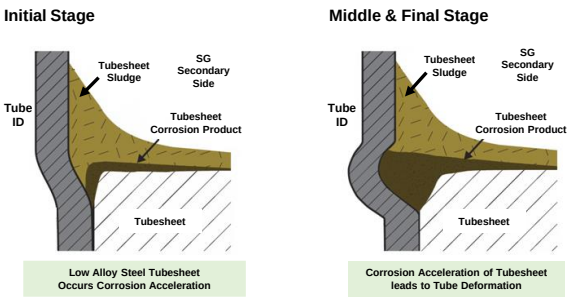

Fig. 1. Schematic of the TTS denting mechanism of SG in nuclear power plants [4].

Denting or tube deformation could lead to outer diameter stress corrosion cracking (ODSCC) in SG tube. This degradation mechanism could be greatly affected by the concentration of impurities such as chloride and sulfate ions and lead, as well as oxidants in the crevices [4].

There are many researches on the effect of deformation on ODSCC of SG tube materials. However, there have been few investigations on the effects of denting or deformation on the general corrosion behavior of SG tube in crevices.

In this work, the effect of plastic deformation on the microstructure and general corrosion behavior of Alloy 690TT tubes was investigated in SG crevice conditions. To simulate the SG crevice condition, the high temperature and high pH compared to normal operation condition, concentration of aggressive impurities such as Na, Cl, S, and Pb were considered.

2. Methods

Commercial Alloy 690TT tube was used for the corrosion tests. The chemical composition of Alloy 690TT tube is presented in Table I. Alloy 690TT specimens were machined in the form of a typical tensile test specimen. The specimens were deformed by about 0, 15%, and 30% using Material Testing System. After that, the specimens were machined into two sizes: A size of 30 mm × 0.5 mm × 1.07 mm for weight change measurement and a size of 20 mm × 0.5 mm × 1 mm for microstructure analysis.

Table I: Chemical composition of Alloy 690TT tube (wt. %).

Cr	Fe	Si	Mn	Ti	Al	C	Ni
29.3	10.4	0.3	0.3	0.3	0.2	0.02	Bal.

Corrosion test was conducted in 1 gallon static autoclave made of Hastelloy C276. To simulate the SG crevices, the solution is the mixed solution with 3 M NaCl, 0.35 M Na_2SO_4, 0.001 M NaOH, and 500 ppm PbO. The pH of test solution is 8.0 at 310 ºC. The test solution was controlled at a dissolved oxygen value of <5 ppb. After the solution temperature was reached at 310 ºC, the corrosion tests were performed for 3000 h. The gravimetric method was used to obtain corrosion rate from the corroded specimens.

Before the corrosion test, the grain size, preferred orientation, Kerneal Average Misorientation (KAM), and dislocation density of specimens were analyzed by the SEM combined with electron back-scatter diffraction (EBSD). Before and after the corrosion tests, the surface and oxide layers of specimens were analyzed using a scanning electron microscope (SEM) and transmission electron microscope (TEM) with energy-dispersive X-ray spectroscopy (EDS).

3. Results

Fig. 2 shows the SEM images of surface of non-deformed and deformed Alloy 690TT specimens before the corrosion test. The surface of non-deformed specimen was generally flat and smooth. No damage or cracks were observed on the surface of non-deformed specimen. However, the some damage or micro-cracks were observed on surface of deformed specimens. As the degree of deformation of specimen increased, the degree of damage and the number of cracks increased. During the plastic deformation process, the surface of Alloy 690TT specimen could be damaged such as strain concentration, void formation, and carbide fracture at grain boundaries [5]. We think that the surface damage and micro-cracks formed on surface of specimen could increase the general corrosion rate of Alloy 690TT specimens.

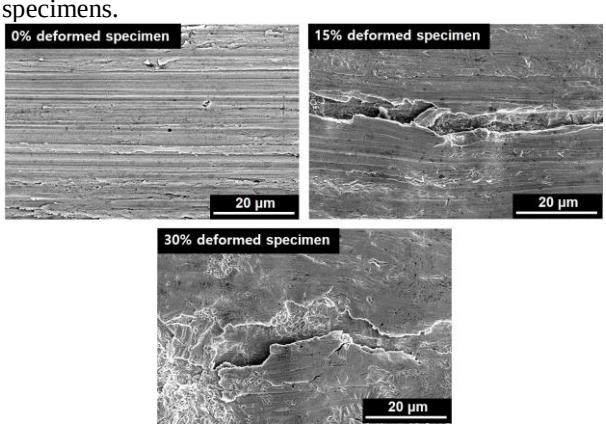

Fig. 2. SEM images of surface of the non-deformed and deformed Alloy 690TT specimens before the corrosion test.

The microstructure of the specimens with different degrees of deformation was characterized by EBSD analysis. Fig. 3 shows the EBSD 001 inverse pole figure (IPF) map of non-deformed and deformed Alloy 690TT specimens. Due to plastic deformation, many grains have been deformed. As shown in Fig. 3, regardless of degree of elongation, a random orientation was observed (predominant orientation color did not appear). In addition, plastic deformation does not significantly affect the size and number of grains.

Fig. 4 shows the KAM map of Alloy 690TT specimens. KAM map indicates that the crystal orientation deviation between a kernel center point and the neighboring points. As shown in Fig. 4, the misorientations of all specimens do not exceed 5°. In the case of non-deformed specimen, KAM map shows blue color. However, KAM map of 15% and 30% deformed specimens has the mixed color with blue, green, yellow, and red. As the elongation of specimen increased, most of them were yellow and red. Average KAM results of three specimens (0%, 15%, and 30% deformed specimens) were 0.11, 1.73, and 2.39°, respectively. As the plastic deformation increased, the average KAM increased because the plastic deformation increases the average direction deviation angle by inducing slip within the microstructure [6].

Using the KAM results, burgers vector, and step size, geometric dislocation density could be calculated. As a results, as the elongation of specimen increased, the geometrically necessary dislocation density increased.

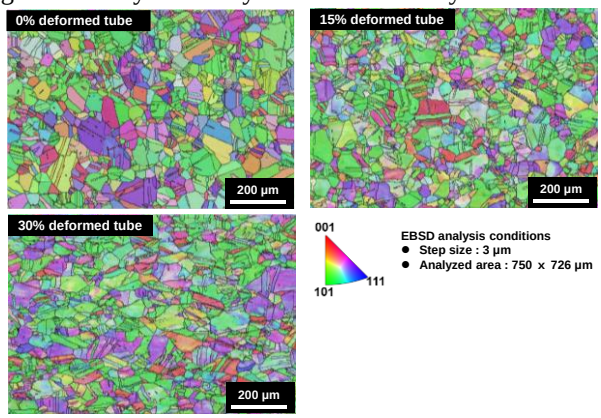

Fig. 3. EBSD IPF of the non-deformed and deformed Alloy 690TT specimens.

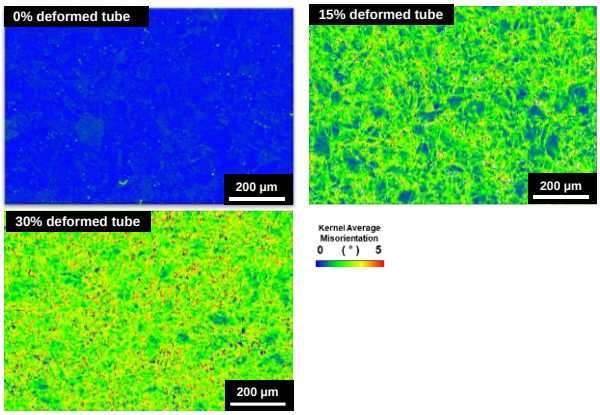

Fig. 4. KAM maps of the non-deformed and deformed Alloy 690TT specimens.

Fig. 5 shows the SEM images of non-deformed and deformed Alloy 690TT specimens after the corrosion test for 1000 h. The plate-like and polyhedral oxide particles were observed under all specimens. However, the oxide particles were more densely formed on the 30% deformed specimen compared to the non-deformed specimen. In the case of 15% and 30% deformed specimen, there is no difference in the size and shape of the oxide particles formed on the damaged and undamaged surfaces. As the elongation of specimen

increased, the number and size of oxide particles formed on specimens increased. Based on the results, it indicated that the corrosion rate of Alloy 690TT specimen increased as the degree of deformation increased.

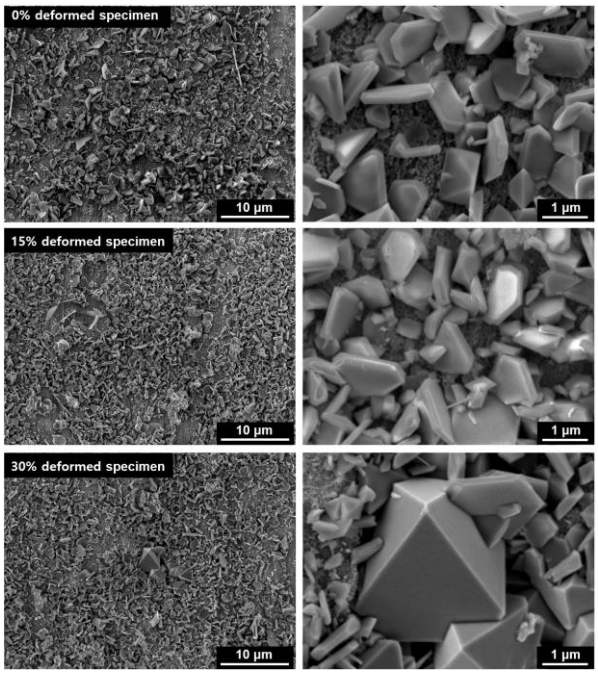

Fig. 5. SEM images of oxide particles formed on surface of the specimens after the corrosion test for 1000 h.

Fig. 6 shows the corrosion rate of non-deformed and deformed Alloy 690TT specimens in SG crevice condition. Under all specimens, the corrosion rate decreased with the increasing time. In the case of 250 h, compared to non-deformed specimen, the corrosion rate of 15% and 30% deformed specimens increased by about 44% and 53%, respectively. In the case of 3000 h, compared to non-deformed specimen, the corrosion rate of 15% and 30% deformed specimens increased by approximately 15% and 31%, respectively. Based on the results, the deformation of Alloy 690TT specimen could greatly affect the general corrosion rate due to the microstructural change.

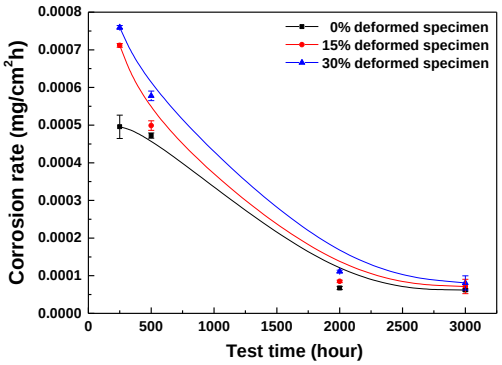

Fig. 6. Corrosion rate of non-deformed and deformed Alloy 690TT specimens in SG crevice condition.

The chemical species of oxide layers formed on Alloy 690TT specimens will be analyzed using the X-ray diffraction and X-ray photoelectron spectroscopy. The details of oxide layer formed on specimens will be presented at the oral presentation.

4. Conclusions

(1) Based on the SEM-EBSD results, the plastic deformation does not affect the size and number of grains. However, the elongation increased, surface defects, average KAM, and geometrically necessary dislocation density increased.
(2) Under all specimens, the plate-like and polyhedral oxide particles were observed. As the elongation of specimen increased, the number and size of oxide particles formed on specimens increased.
(3) The general corrosion rate of Alloy 690TT tube increased with increasing the degree of plastic deformation owing to the microstructural change.
(4) In the future work, we will perform the electrochemical tests to evaluate the stability of passive film formed on non-deformed and deformed Alloy 690TT specimens.

ACKNOWLEDGEMENTS

This work was supported by the National Research Foundation (NRF) grant funded by the Korean government (NRF-2021M2E4A1037979 and RS-2022-00143316).

REFERENCES

[1] D. Curieres, I. Environmental degradations in PWR steam generators. In Steam Generators for Nuclear Power Plants; Woodhead Publishing: Cambridge, UK, 2017.
[2] S. Choi, PWR steam generator tube denting at top of tubesheet. Paper 10137. In Proceedings of the International Conference on Nuclear Power Chemistry, Sapporo, Japan, p. 26–31 October. 2014.
[3] R.W. Staehle, J.A. Gorman, Quantitative assessment of submodes of stress corrosion cracking on the secondary side of steam generator tubing in pressurized water reactors: Part1. Corrosion, Vol.59, p. 931–944, 2003.
[4] R. Wolfe, H. Feldman, Steam Generator Management Program: PWR Steam Generator Top-of-Tubesheet Denting, EPRI TR-3002002197, 2014.
[5] Q.J. Peng, J. Hou, T. Yonezawa, T. Shoji, Z.M. Zhang, F. Huang, E.-H. Han, W. Ke, Environmentally assisted crack growth in one-dimensionally cold worked Alloy 690TT in primary water, Corrosion Science, Vol.57, p. 81-88, 2012.
[6] M. Kamaya, Angus J. Wilkinson, John M. Titchmarsh, Quantification of plastic strain of stainless steel and nickel alloy by electron backscatter diffraction, Acta Materiallia Vol.54, p. 539–548, 2006.